Vision Research 50 (2010) 585–597

Contents lists available at ScienceDirect

Vision Research

journal homepage: www.elsevier.com/locate/visres

A model of plaid motion perception based on recursive Bayesian integration of the 1-D and 2-D motions of plaid features

Kameliya D. Dimova, Michael J. Denham *

Centre for Theoretical and Computational Neuroscience, University of Plymouth, Plymouth PL4 8AA, UK

ARTICLE INFO

Article history:
Received 30 September 2009
Received in revised form 28 December 2009

Keywords:
Plaid
Motion
Bayes
Computational model
Blobs

ABSTRACT

We describe a theoretical and computational model of the perception of plaid pattern motion which fully accounts for the majority of cases in which misperception of the direction of motion of Type II plaids has been observed [Yo, C., & Wilson, H. (1992). Perceived direction of moving two-dimensional patterns depends on duration, contrast, and eccentricity. *Vision Research 32*, 135–147]. The model consists of two stages: in the first stage local motion detectors signal both the one-dimensional (1-D) and two-dimensional (2-D) motion of the high luminance features (blobs) in the plaid pattern; in the second stage these local motion signals are combined using a recursive Bayesian least squares estimation process. We demonstrate both theoretically and using simulations of the computational model that the estimated direction of the plaid motion for Type II plaids is initially dominated by the 1-D motion of the longer edges of the elongated blobs, which is in a direction close to the vector sum direction of the component gratings. The recursive estimation process which combines the local motion signals in the second stage of the model results in a dynamic shift in the estimated plaid direction towards the direction of the 2-D motion of the blobs, which corresponds to the veridical plaid direction.

1. Introduction

The problem of how the visual system combines the motion of two moving gratings to form the percept of a coherent moving plaid pattern is still unsolved after nearly 30 years of research. It has long been known that the plaid motion can be computed by a velocity space construction, known as the intersection-of-constraints (IOC) (Fennema & Thompson, 1979). Based on this, Adelson and Movshon (1982) proposed a two-stage model for the analysis of plaid motion in which the one-dimensional (1-D) motions of the plaid's two component gratings are first determined, and then combined in a weighted summation corresponding to the IOC construction. This model has dominated research in the area for almost 30 years, despite the psychophysical (Derrington & Badcock, 1992; Derrington & Suero, 1991; Stone, Watson, & Mulligan, 1990; Welch, 1989) and physiological (Movshon, Adelson, Gizzi, & Newsome, 1985; Movshon & Newsome, 1996; Tinsley et al., 2003) evidence being equivocal. In particular, the available evidence is based entirely on experiments using symmetric Type I plaids (Ferrera & Wilson, 1990), for which the plaid velocity vector lies between the velocity vectors of the two component gratings, which have equal magnitude. The strongest evidence against the Adelson and Movshon (1982) model was obtained when Type II plaids, the velocity vector of which lies outside of the velocity vectors of the two component gratings, were used in psychophysical experiments (Yo & Wilson, 1992). These experiments demonstrated that the direction of the plaid motion during the initial period (up to ~60 ms) of stimulus presentation is misperceived, with a strong bias in the perceived direction towards the vector sum (*VS*) of the velocities of the component gratings. Whilst it is possible that the Adelson and Movshon (1982) model is correct for Type I plaids, and that another mechanism is responsible for Type II plaid motion perception, this would seem highly unlikely.

Subsequent to the Yo and Wilson (1992) experiments, and prior experiments which showed identified misperceptions in the direction and speed of Type II plaids (Ferrera & Wilson, 1990, 1991), several models have been proposed which attempt to explain these misperceptions. Wilson, Ferrera, and Yo (1992) suggested a model, subsequently extended by Wilson and Kim (1994), which consisted of two parallel processing pathways, one signalling the direction of the component gratings (presumed to be mediated by neurons in area V1 of visual cortex) and the other (presumed to be end-stopped neurons in area V2) signalling, after a hypothesised delay of ~77 ms, the direction of "the motion of illusory lines formed by the nodes of the Type II pattern" (Yo & Wilson, 1992). The signals of the first pathway are combined (by neurons in extrastriate area MT to which both V1 and V2 neurons project) to form a cosine-weighted sum of the component grating velocities. The signals of the second pathway are derived after full-wave rectification of

* Corresponding author.
E-mail addresses: mdenham@plym.ac.uk, michaeldenham@btinternet.com (M.J. Denham).

0042-6989/$ - see front matter © 2010 Elsevier Ltd. All rights reserved.
doi:10.1016/j.visres.2010.01.004

the stimulus and orientation filtering at a lower spatial frequency than that of the component gratings (postulated to take place in V2). A cosine-weighted sum of the two pathways is then followed by competitive feedback inhibition in order to predict the perceived plaid direction. The delay in the second pathway accounts for the initial misperception of the plaid direction towards the vector sum direction of the component gratings' velocities. Whilst this model offers a compelling explanation of the observed misperception, it is deficient in several respects, as discussed in Alais, Wenderoth, and Burke (1997), who carried out experiments on the effect of the size and number of plaid features, or blobs, the "nodes of the Type II pattern" referred to above, on the misperception. They concluded that a more likely explanation is based on "a feature-sensitive mechanism which responds to the motion of plaid features and which is tuned to their various qualities" (Alais et al., 1997). The plaid blobs which they examined and refer to are the high luminance regions which are formed at the intersection of the component gratings and which, in particular for Type II plaids, are the most visually salient features in the plaid pattern for a human observer.

In this paper we show that the misperception of the plaid direction, its dependence on the angular separation and contrast of the component gratings, and its decrease with lengthening stimulus duration, can all be fully explained by a two-stage model which is based on the detection of both the one-dimensional (1-D) and two-dimensional (2-D) motion of the blobs, and their combination by a recursive Bayesian velocity estimation process.

In the first stage of our proposed model, local motion detectors respond to both the 1-D and 2-D motion of the blobs within the plaid. We hypothesise that these detectors are based on the complex and hypercomplex (end-stopped) neurons in V1 (Hubel & Weisel, 1965; Pack, Livingstone, Duffy, & Born, 2003). This stage of the model differs from that of Wilson et al. (1992) in that: (i) the 1-D motion signals are derived not from the motion of the component gratings but from the edge motion of the blobs; (ii) there is no requirement for the separate combination or any explicit weighting, cosine or otherwise, of the 1-D signals; (iii) the 2-D motion signals are derived directly from the terminations (endpoints) of the blobs, without the requirement for full-wave rectification (or squaring) of the plaid stimulus. In the second stage of the model, the 1-D and 2-D motion signals are combined using a recursive Bayesian least squares estimation process, which we postulate to occur in the recurrent V1–MT circuitry. This also differs from the Wilson et al. (1992) model in that cosine weighting of the 1-D and 2-D signals is not required, nor is there the need for a final stage of competitive inhibition.

In the remainder of the paper, we first examine in detail the specific geometric properties of the blobs which, we claim, play the main role in the perception of plaid motion. In particular we show that the shape of the blobs, specifically the extent of their elongation, is defined by the angular difference in the directions of motion of the component gratings, and that the orthogonal direction of motion of the longer edges of the elongated blobs is given by the mean of the directions of motion of the component gratings. We also show that as the blobs become more elongated, the orthogonal direction of motion of the longer edges of the blobs tends towards the vector sum of the directions of motion of the component gratings. Although the blobs have been implicated in the perceptual process by several authors (Alais, Wenderoth, & Burke, 1994; Alais et al., 1997; Burke & Wenderoth, 1993; Wenderoth, Alais, Burke, & van der Zwan, 1994; Wilson et al., 1992), as far as we are aware this is the first time that the geometric properties of the blobs and their relationship to the directions of motion of the component gratings have been precisely defined. Related plaid features and their properties have been described by Bowns (1996, 2006), with similar properties, and we compare these in our discussion (Section 4) with the blob features which we have defined.

Next we show theoretically how these particular properties of the blobs can be used to predict the misperception of the direction of Type II plaids which has been observed psychophysically (Bowns, 1996; Burke & Wenderoth, 1993; Yo & Wilson, 1992). To demonstrate this more fully, we use a computational version of our model to simulate the observed misperception, and show that the magnitude of the direction bias, its dependence on angular separation and contrast, and the convergence of the perceived plaid direction towards the veridical direction with increasing stimulus presentation duration, are all accurately predicted by the model.

Finally we discuss how our model differs from the two-stage model of Adelson and Movshon (1982), yet is consistent with the available physiological and psychophysical evidence, and how it relates to a recent Bayesian extension of the Adelson and Movshon model (Weiss & Adelson, 1998; Weiss, Simoncelli, & Adelson, 2002), and the models proposed by Bowns (1996, 2006).

2. Model description

2.1. Geometric analysis of the plaid blobs

The high luminance regions of the plaid, i.e. the blobs, which are formed at the intersections of the component gratings, can be precisely defined by representing the plaid as the *product* of two gratings rather than as a *sum* of two gratings, its normal form of representation. Typically a plaid is described by the sum of two sine or cosine gratings, i.e. the spatiotemporal luminance intensity function of the stimulus is defined by

$$I(x,y,t) = \sin(\omega_1) + \sin(\omega_2) \quad (1)$$

where $\omega_i = 2\pi s_i(x\cos\theta_i + y\sin\theta_i + r_i t)$; s_i = spatial frequency (cycles/°); θ_i = direction of motion (°); and r_i = speed (°/s), for the ith. grating, $i \in \{1,2\}$. Using a simple trigonometric identity, this expression can be rewritten as,

$$I(x,y,t) = 2\sin((\omega_1+\omega_2)/2)\cos((\omega_1-\omega_2)/2) \quad (2)$$

i.e. as the product of two anti-phase gratings, henceforth referred to as the *product* gratings to distinguish them from the *component* gratings used in the summation form (1) of the plaid. The two product gratings comprise: (i) a sine grating which moves in the direction $\phi = (\theta_1+\theta_2)/2$, and which has a spatial frequency $s_\phi = (s_1\cos\theta_1 + s_2\cos\theta_2)/2\cos\phi$, and a speed $r_\phi = (r_1+r_2)\cos\phi/(\cos\theta_1+\cos\theta_2)$; and (ii) a cosine grating which moves in the direction $\varphi = \phi - 90°$, has a spatial frequency $s_\varphi = (s_1\cos\theta_1 - s_2\cos\theta_2)/2\cos\varphi$, and a speed $r_\varphi = (r_1-r_2)\cos\varphi/(\cos\theta_1-\cos\theta_2)$. For simplicity we have assumed henceforth that $s_1 = s_2 = s$.

Derrington and Ukkonen (1999) used this representation to describe a specific instance of a plaid with component gratings oriented symmetrically about the vertical and a specific relationship between the spatial frequency of the gratings and their orientations. In this case they obtain a vertically oriented, horizontally moving product grating and horizontally oriented, stationary product grating.

Fig. 1a–c shows three examples of equivalent plaid representations in terms of their component and product gratings. These clearly demonstrate that the high luminance regions, or blobs, in the plaid which occur at the intersections of the component gratings are precisely defined by the anti-phase modulation of one product grating by the other. In particular, where the spatial frequencies of the product gratings differ substantially (Fig. 1a and c), the blobs are readily seen to correspond to the high luminance bands of the higher frequency product grating modulated by the lower frequency product grating. The shape of the blobs, in terms of the ratio of their long and short edges, is thus determined by the ratio of the spatial frequencies of the product gratings, which

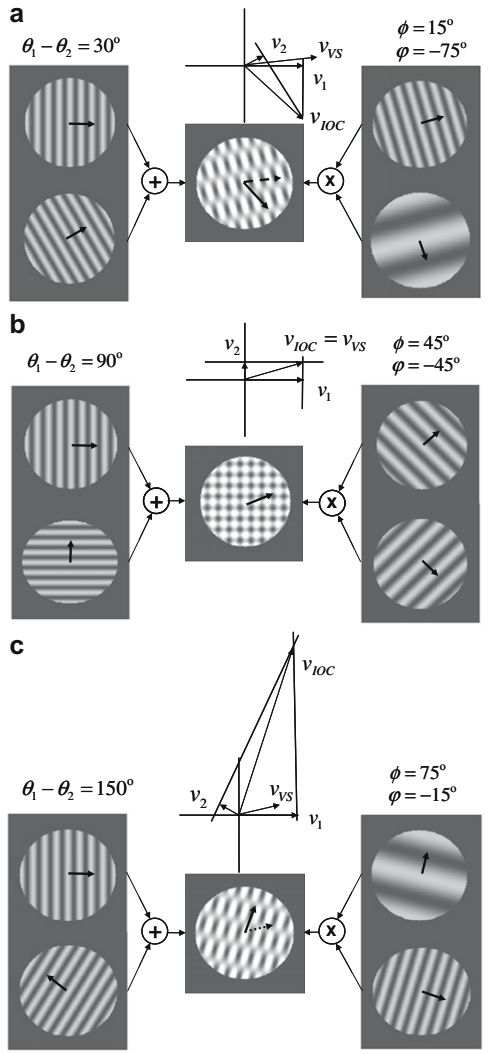

Fig. 1. Three examples (a–c) of the representation of a plaid (centre) as the sum (left) or the product (right) of two gratings. The velocity space diagram above each plaid shows the velocity vectors for each component grating, v_1 and v_2 together with the IOC and vector sum velocity vectors v_{IOC} and v_{VS}. The arrows on the gratings and plaids also show their directions of motion, with the dashed arrow on the plaid showing the vector sum direction.

can be expressed in terms of the angular difference $\theta_1 - \theta_2$ in the directions of the component gratings as

$$s_\phi / s_\varphi = 1/\tan((\theta_1 - \theta_2)/2) \quad (3)$$

The direction of motion of the blobs (and therefore the IOC direction of the plaid) is given by the vector sum direction of the two *product* gratings.

We are mostly concerned here with Type II plaids (e.g. Fig. 1a), so in order to simplify the presentation we will derive the main characteristics of the blobs only for this case, although similar equations describing the characteristics of Type I plaids (e.g. Fig. 1b and c), can be easily obtained. For the Type II property, that the IOC velocity vector lies outside of the two component grating velocity vectors, to hold the ratio of the speeds of the component gratings, r_1/r_2, must be greater than one, and the difference in their directions of motion, $\theta_1 - \theta_2$, must be less than 90°. It follows from (3) that, as the difference in the direction of motion of the two component gratings, $\theta_1 - \theta_2 < 90°$, decreases, the ratio of the spatial frequencies of the product gratings, s_ϕ/s_φ, will increase, and the blobs will become more elongated in shape. Moreover, the shape of the blobs only depends on the difference between the directions of the two component gratings, $\theta_1 - \theta_2$, and not on the ratio of their speeds. It also follows from (3) that $s_\phi > s_\varphi$, and thus the motion of the longer edges of the blobs orthogonal to their orientation will be in the direction $\phi = (\theta_1 + \theta_2)/2$, the mean of the directions of motion of the component gratings.

Most importantly, we can express the difference between the orthogonal direction of motion of the longer blob edges, ϕ, and the vector sum direction of the two component gratings, denoted by θ_{VS}, as

$$\phi - \theta_{VS} = \arctan\left(\frac{(r_1/r_2) - 1}{(r_1/r_2) + 1} \cdot \frac{s_\varphi}{s_\phi}\right) \quad (4)$$

This shows that, for a fixed ratio of component grating speeds, r_1/r_2, as the difference between directions of the two component gratings, $\theta_1 - \theta_2$, decreases, and the shape of the blobs become more elongated, the angular difference between the orthogonal direction of motion of the longer blob edges and the vector sum direction of the component gratings will decrease. It is also worth noting that for a fixed difference in the directions of the component gratings, $\theta_1 - \theta_2$, as the speed ratio r_1/r_2 increases, the angular difference expressed by (4) will increase, causing the orthogonal direction of motion of the longer edges of the blobs to move away from the vector sum direction of the component gratings.

2.2. Theoretical predictions of the model

The geometric analysis of the blobs, as expressed by Eqs. (2)–(4), allow us to make theoretical predictions about the behaviour of our model in response to Type II plaids. In the first stage of the model, we propose that local motion detectors signal both the 1-D (edge) and 2-D (end-point) motion of the blobs present within the plaid. Thus in the case of Type II plaids, for which the blobs are elongated, the majority of the local motion detectors will respond to the 1-D motion of the longer edges of the blobs. Since a local motion detector signals the velocity of 1-D edge motion in the direction orthogonal to the orientation of the edge, owing to the aperture effect (Marr & Ullman, 1981; Wallach, 1935; Wuerger, Shapley, & Rubin, 1996), the majority of the local motion detectors will signal motion in the orthogonal direction of motion of the long edges of the blobs. The geometric analysis of the previous section shows that for a fixed ratio of component grating speeds, r_1/r_2, as the difference between the directions of the two component gratings, $\theta_1 - \theta_2$, decreases and the shape of the blobs become more elongated, the orthogonal direction of motion of the longer edges of the blobs, ϕ, will tend towards the vector sum direction of the component gratings. Thus the majority of the local motion detectors will signal motion in a direction which is increasingly biased, as $\theta_1 - \theta_2$ decreases, towards the vector sum direction of the component gratings.

In the second stage of the model, we propose that the outputs of the local motion detectors are combined using a recursive Bayesian estimation process. The estimate computed in the first iteration of the estimation process will thus form the model's prediction of the perceived plaid velocity in a short initial period of stimulus presentation. As we have already discussed, this estimate will be dominated by the majority of local motion detectors which signal the orthogonal motion of the blobs in the ϕ direction. We have also shown, in Eqs. (3) and (4) respectively, that as the difference between component grating directions, $\theta_1 - \theta_2$, decreases: (i) the long edge of the blob will become longer and therefore drive an increasing majority of local motion detectors; and (ii) the orthogonal motion of the blobs in the ϕ direction approaches the vector sum direction of the component gratings. Hence it follows that, as the angle between the component gratings decreases, the first

velocity estimate formed by the model, and therefore the initial plaid velocity predicted by the model, will be increasingly biased towards the ϕ direction, which itself will approach the vector sum direction of the component gratings. This is precisely what Yo and Wilson (1992) observed in their psychophysical experiments.

For example, consider one of the Type II plaids used by Yo and Wilson in their experiments. The parameters of the component gratings of this plaid are: $\theta_1 = 70.5°$, $\theta_2 = 48.2°$, $r_1 = 1.33$, and $r_2 = 2.67$. Then, for these values: $\theta_1 - \theta_2 = 22.3°$, $\theta_{IOC} = 0.2°$, $r_{IOC} = 3.9$, $\theta_{VS} = 55.6°$, $r_{VS} = 4.0$, $\phi = 59.4°$, $\phi - \theta_{VS} = 3.8°$ and $s_\phi / s_\varphi = 5.1$. The blobs are thus elongated (edge ratio of 5:1) and move orthogonally to their longer edges in a direction which is less than 4° from the vector sum direction of the component gratings. In Yo and Wilson's experiment, the perceived direction of the plaid motion in the initial period of presentation was observed to be approximately 60°. This is close to the vector sum direction of 55.6°, and almost exactly equal to the orthogonal direction $\phi = 59.4°$ of motion of the longer edges of the blobs.

The velocity estimate formed by the model during subsequent iterations of the recursive estimation process will also be influenced by the majority of local motion detectors which signal the orthogonal direction ϕ of the longer edges of the blobs, although this influence will gradually decrease with each iteration (see the simulation model description below) leading to convergence to a steady-state velocity estimate. Thus for long stimulus presentations the perceived direction of the plaid motion predicted by the model will continue to be biased, but to a lesser extent, in the direction $\phi = (\theta_1 + \theta_2)/2$, the mean of the component gratings' directions. This is precisely what Ferrera and Wilson (1990) observed, i.e. that the perceived direction of the plaid motion has a small residual bias, after approximately 150 ms of presentation time, of between 8° and 10° towards the mean of the component gratings' directions, in this case for plaids with component grating separations of between 22.3° and 51.6°. A similar residual bias was observed by Burke and Wenderoth (1993). They found in addition that as the difference in component grating directions decreased from 40° to 10°, the residual bias increased from 2° to 17°. This dependence of the residual bias on the difference in component grating directions was observed for a constant value of $\phi = (\theta_1 + \theta_2)/2$. Hence they argued that the bias could not be due to the orthogonal direction of motion of the elongated blobs which remained constant in this experiment. In our model however the strength of both the initial and the residual bias is determined by the length of the long edges of the blobs, since this determines the number of local motion detectors which signal the orthogonal 1-D motion of the blob edges in the ϕ direction. Since the elongation of the blobs increases with decreasing difference in the direction of motion of the component gratings, as shown by Eq. (3), it follows that the residual bias will always be towards the ϕ direction, but will increase as the difference in component grating directions decreases.

The theoretical predictions of the model, presented above, are largely qualitative in nature, but will be confirmed in a more quantitative form in Section 3 of the paper, where we describe the results from using of a computational version of our model to simulate the perceptual experiments of Yo and Wilson (1992), Bowns (1996) and Burke and Wenderoth (1993). The form of the computational model is described in the next section.

2.3. Computational model description

To quantify the predictions of our model and, in particular, to demonstrate the convergence of the estimated direction of the Type II plaid motion towards the true IOC direction, we will use a computational version of the model to simulate the psychophysical experiments of Yo and Wilson (1992) and Burke and Wenderoth (1993).

A detailed description of the model has been given previously (Dimova & Denham, 2009), where the model was used to explain the initial direction bias in the velocity of smooth eye pursuit eye movements (Masson & Stone, 2002; Wallace, Stone, & Masson, 2005). Briefly, the input to the model is the luminance function $I(x, y, t)$ of Eq. (1), describing the plaid pattern and its motion, which is presented in a 200×200 pixel visual space. Local motion detectors measure the spatial and temporal derivatives I_x, I_y, I_t of $I(x, y, t)$ in a number of 10×10 pixels, non-overlapping windows uniformly distributed across the visual space, using a simple spatial and temporal shift mechanism. These measurements are then related to the pattern velocity vector $\begin{bmatrix} v_x \\ v_y \end{bmatrix}$ by the gradient-based equation (Fennema & Thompson, 1979):

$$I_t = [I_x \quad I_y] \begin{bmatrix} v_x \\ v_y \end{bmatrix} + \eta \tag{5}$$

where η is additive zero mean, normally distributed measurement noise. A recursive algorithm, well-known as the Kalman filter (Kalman, 1960), is used to determine a least squares estimate of the velocity vector based on the set of measurements from the local motion detectors, as the best-fit solution to the corresponding set of gradient-based Eq. (5). The velocity estimate in the estimation algorithm is initialised to zero, which corresponds assigning a zero mean, *a priori* velocity distribution in the Bayesian formulation of the estimation algorithm.

As we have described, the bias in the first velocity estimate formed by the model results from the large number of local motion detectors for which the measured derivatives I_x, I_y, I_t correspond to the 1-D motion of the longer edges of the blobs. For these detectors many solutions to the corresponding gradient-based Eq. (5) are possible, corresponding to the aperture effect (Marr & Ullman, 1981; Wallach, 1935; Wuerger et al., 1996). The zero-valued initial velocity estimate provides a constraint on the estimate formed by the first step of the algorithm, which results in an best-fit solution being selected for which the magnitude of the velocity estimate is smallest. This corresponds to the solutions to (5) for each local motion detector for which the selected velocity is in the direction orthogonal to the longer edges of the blobs. Thus the estimate formed in the first step of the algorithm will be strongly biased in this direction, with the strength of the bias dictated by the number of motion detectors signalling the direction. As we have shown, the bias will be stronger as the difference between the directions of the component gratings decreases, since this results in a greater elongation of the blobs.

In contrast, measurements of I_x, I_y, I_t from the local motion detectors which signal the 2-D motion of the end-points of the blobs result in a unique (within the noise) solution to the corresponding set of gradient Eq. (5). This solution corresponds to the vector sum direction of the *product* gratings, and thus, equivalently, to the veridical, IOC direction of the plaid. These local motion detectors will therefore influence the estimate of plaid direction towards the IOC direction, both in the initial step of the algorithm and in all further steps. However, lowering the contrast of the plaid stimulus, or equivalently reducing the signal to noise ratio in Eq. (5), will result in a weaker influence of this solution, and thus allow a greater bias in the estimated direction of the plaid towards the vector sum direction of the *component* gratings.

As the number of iterations of the recursive estimation algorithm increases, the effect of the 1-D local motion detectors will decrease in relation to that of the 2-D motion detectors, since the velocity estimate formed in each iteration of the algorithm becomes the prior estimate for the next iteration. This gradually relaxes the effect of the zero prior constraint on the solution to (5)

corresponding to the set of outputs of the 1-D motion detectors, allowing the solution to (5) corresponding to the set of outputs of the 2-D motion detectors to increasingly influence the velocity estimate at each iteration.

In the following section we will show by simulations of the computational version of the model that, in accordance with the above theoretical predictions, the model also yields quantitative predictions of the perceived direction of plaid motion which closely resemble the experimentally obtained data of Yo and Wilson (1992), Bowns (1996) and Burke and Wenderoth (1993).

3. Simulation results

3.1. Simulation of the Type II plaid experiments of Yo and Wilson (1992) and Bowns (1996)

In Fig. 2a–f, we show the results obtained using the computational model to simulate the psychophysical experiments of Yo and Wilson (1992) and Bowns (1996). Yo and Wilson (1992) used as stimulus three different Type II plaids (see their Fig. 2), although the results were not given for all three plaids for each of the experiments. The main experiments, which we simulate here, observed the perceived direction of plaid motion as functions of presentation duration and pattern contrast. Their results on presentation duration are given for the plaid with the following parameters: $\theta_1 = 70.5°$, $\theta_2 = 48.2°$, $r_1 = 1.33$, $r_2 = 2.67$, $s_1 = s_2 = 1.5$, $\theta_1 - \theta_2 = 22.3°$, $\theta_{IOC} = 0.2°$, $r_{IOC} = 4.02$, $\theta_{VS} = 55.6°$, $r_{VS} = 3.93$. For the product plaid representation, these parameters give: $\phi = 59.4°$, $\phi - \theta_{VS} = 3.8°$, $r_\phi = 2.0$, $r_\varphi = 3.5$, $s_\phi = 1.5$, $s_\varphi = 0.3$ and $s_\phi/s_\varphi = 5.0$. Note that both the speed and spatial frequency of the higher spatial frequency product grating are similar to those of the component gratings.

For this plaid, two observers reported a perceived direction of motion of approximately 60° after 60 ms of presentation, reducing to approximately 15° and 30° respectively after 90 ms, and to approximately 0° (the IOC direction) after 150 ms. Note that the reduction in the bias was apparently gradual rather than occurring discontinuously as might be expected if additional 2-D motion information became available after some fixed time delay, as was

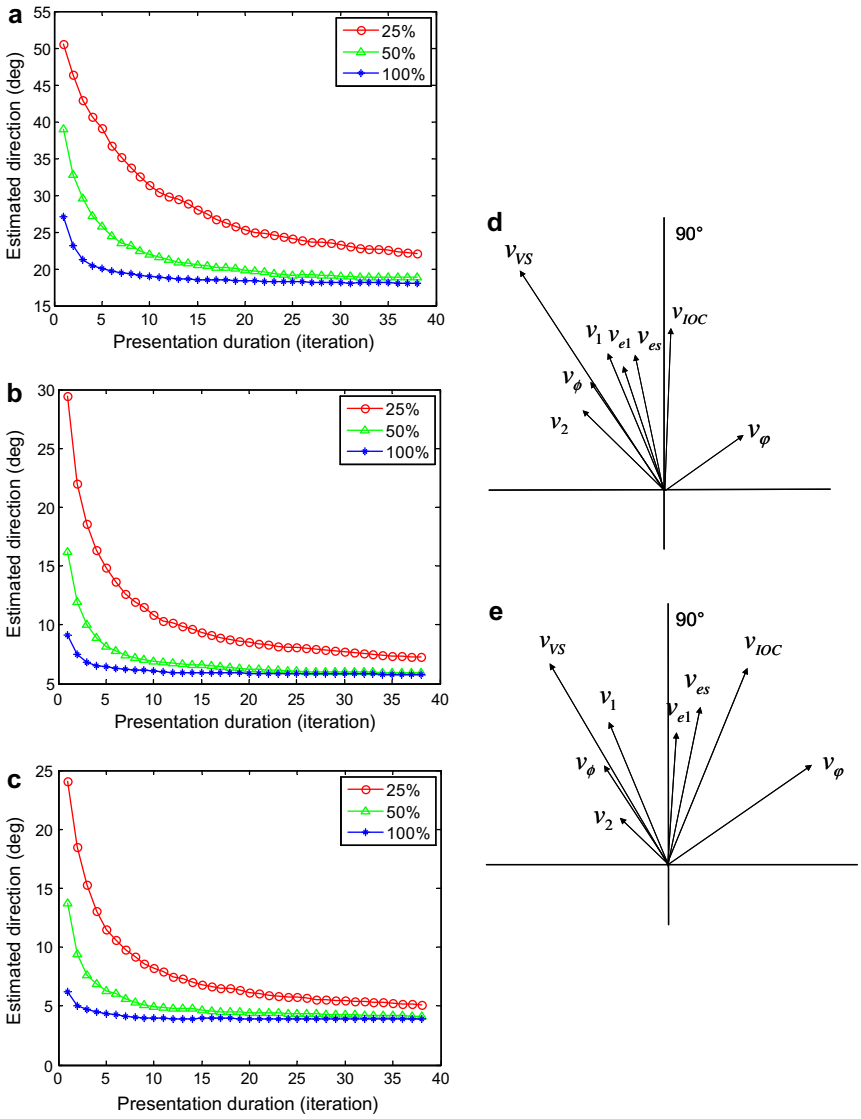

Fig. 2. (a–c) Simulations of the computational model for three cases of Type 2 plaids used in the experiments of Yo and Wilson (1992): (a) $\theta_1 = 70.5°$, $\theta_2 = 48.2°$, $r_1 = 1.33$, $r_2 = 2.67$, $\theta_{IOC} = -0.2°$, $\theta_{VS} = 55.6°$; (b) $\theta_1 = 84.3°$, $\theta_2 = 36.9°$, $r_1 = 0.25$, $r_2 = 2$, $\theta_{IOC} = 0°$, $\theta_{VS} = 41.7°$; (c) $\theta_1 = 85.2°$, $\theta_2 = 33.6°$, $r_1 = 0.4$, $r_2 = 4$, $\theta_{IOC} = 0°$, $\theta_{VS} = 37.8°$, and for three different stimulus contrast levels. The results illustrate the dependence on stimulus contrast of the initial and final estimates of plaid direction, and of the convergence rate of the estimate towards the true IOC plaid direction. Presentation duration is represented by the number of iterations of the algorithm. (d and e): Vector space diagrams showing the model simulation results for Experiment 3 of Bowns (1996). The initial v_{e1} and final v_{es} plaid velocity estimates from our model are shown together with the component grating velocity vectors v_1 and v_2, and the vector sum and IOC velocity vectors.

suggested in the Wilson et al. (1992) model. When the plaid contrast was varied, with values of 5%, 50% and 100%, the observed initial bias at 60 ms was 60°, 40° and 30° respectively, and the length of time for the bias to reduce lengthened considerably with decreasing contrast. For a contrast of 5–10%, a substantial bias of approximately 25° was observed after 1 s of presentation.

We can compare these experimental results with the graph shown in Fig. 2a, which shows the model results for this plaid. As the graph shows, the bias in the estimated direction at the first iteration for the three values of contrast, 25%, 50% and 100%, are remarkably similar to the initial perceived bias observed experimentally. We note also that the convergence time decreases substantially with increasing contrast, and that there is a considerable steady-state bias for all contrasts of up to 25° for this plaid, again as observed experimentally. Fig. 2b and c show the same simulations for the other two plaids used by Yo and Wilson (1992), but for which they did not report the results as fully as for the first plaid. These graphs show similar characteristics of the variation in magnitude and convergence rate of the direction bias with contrast as in Fig. 2a, but with the steady-state bias reducing with increasing difference in the directions (47.4° and 51.6° respectively) of the component gratings in Fig. 2b and c, to between 4° and 10°. In Ferrara and Wilson (1990), the perceived steady-state bias for similar Type II plaids was approximately 6°.

In Bowns (1996), a number of experiments were carried out which attempted to establish whether or not the misperception of the plaid direction observed by Yo and Wilson (1992) generalises to all Type II plaids and is due to a temporal delay in Fourier and non-Fourier motions processing as proposed in the parallel pathway model of Wilson et al. (1992). Here we have simulated their Experiment 3 which used Type II plaids very similar to those used by Yo and Wilson (1992). The component gratings for these plaids had the same spatial frequencies (1.3 cycles/°) and orientations (202° and 225°) but differed in the ratio of their speeds, which ranged from 1:0.45 to 1:0.75, with the speed of one of the component gratings held constant at 3.13 °/s. The experiments used a simple forced choice response which required subjects to report either a plaid direction to the right or to the left of "the vertical", i.e. 90°. The component grating directions and speeds were such that the vector sum direction remained virtually constant, varying from 29° to 32° to the left of the vertical, for the varying speed ratios, whereas the IOC direction varied from 28° to 2° to the right of the vertical.

The experiments revealed that for the two speed ratios at the extreme ends of the above range, subjects reported a perceived direction of plaid motion which shifted from 100% in the vector sum direction (i.e. left of vertical), for a speed ratio of 1:0.75, to 100% in the IOC direction (i.e. right of vertical), for a speed ratio of 1:0.45. This was interpreted in Bowns (1996) as: "a rather surprising complete reversal of the perceived motion in the direction of the IOC".

We simulated the cases of the two plaids at the extremes of the ranges of speed ratios referred to above. The experimental data was also simulated by Weiss and Adelson (1998) – see our discussion of their model in Section 4. The simulation results from our model are described in Fig. 2d (for a speed ratio of 1:0.75) and 2e (for a speed ratio of 1:0.45) in the form of vector space diagrams. As these Figures show, changing the ratio of the component grating speeds from 1:0.75 to 1:0.45 is sufficient to move the both the estimate formed in the first step of the estimation algorithm, v_{e1}, and the steady-state estimate, v_{es} of the perceived plaid direction from being on the left of the vertical (vector sum side) to being on the right of the vertical (IOC side).

The difference in the directions of the first step velocity estimate v_{e1} for the two speed ratios is 21° (108° vs. 87°). However the difference in the first step direction bias estimate (relative to the IOC direction) is only 5° (20° from IOC vs. 25°). For the steady-state velocity estimate v_{es}, the estimated direction differs by 24° (102° vs. 78°) for the two speed ratios, but the difference in the estimated bias is only 2° (14° from IOC vs. 16°).

Thus the change in the estimated bias is small with this change in speed ratio, both in the first step of the algorithm and after convergence, and we suspect that the change in the perceived bias is also small. The simple forced choice response of left or right of the vertical appears however to have resulted in an interpretation in Bowns (1996) that there is a large change in bias which leads to a reversal in the perception of the plaid motion direction from the IOC to the vector sum direction.

We suggest an alternative interpretation, supported by our simulation results (see Fig. 2d and e), that the value of the perceived bias for the two speed ratios is almost the same, but that the change in speed ratio results in a shift in the IOC direction towards the vector sum direction, causing the perceived motion direction to switch from right side of the vertical to the left side.

In the Section 4 we will describe also our simulation results for the set of plaids used in Experiment 2 of Bowns (1996), with angular differences between component gratings in a range between 10° and 90°, and a speed ratio of 1:0.5.

3.2. Simulation of the experiments of Burke and Wenderoth (1993)

In Fig. 3, we show the results obtained using the computational model to simulate the psychophysical experiments of Burke and Wenderoth (1993), in which they used Type II plaids to study the dependence of the steady-state misperception of plaid direction on the angular difference between the component grating directions. The plaids were constructed using component gratings with angular differences of 10°, 20°, 30° and 40°. The true plaid direction was 270° and the stimulus was presented for 10 s. Two experiments were carried out: in the first, the component directions were chosen so that the mean was constant at 295°; in the second, one component direction was kept constant at 315°. Fig. 3a and b show the results from each experiment, both the perceived plaid direction obtained in the Burke and Wenderoth (1993) study (▲ symbols) and the direction estimated by the model (● symbols). In Fig. 3a the mean component direction is 295°, and in Fig. 3b this direction varies and is shown by the dashed line.

The graphs in Fig. 3 show that the estimated plaid direction from the model simulation varies with the difference in component grating direction and displays in both cases the same trend in the variation as observed in the Burke and Wenderoth (1993) study, although with a slightly greater bias towards the mean component direction of up to 9°. Importantly the model shows in Fig. 3b the same non-linear variation of the estimated direction with component separation as was observed experimentally for the perceived direction.

3.3. Robustness of the model

In the above cited experiments and those that are described later in the Section 4, the stimuli were presented in a circular windows with the following diameters: Yo and Wilson (1992) – diameter = 8°; Bowns (1996) – diameter = 3°; Stone et al. (1990) – diameter = 5.4°; Champion, Hammett, and Thompson (2007) – diameter = 6°; Alais et al. (1997) – diameter = 3°, 6° and 12°. We do not have any information on the size of the stimulus used in the experiments of Burke and Wenderoth (1993). In the simulations described in Section 3.2 and in the Section 4, we display the image in a circular aperture of diameter 200 pixels; thus the size of our 10×10 pixel window corresponds to between 0.15° and 0.6°. This is in close accordance with an average receptive field diameter measurement, for V1 cells in humans, of approximately 0.25° at the fovea, rising linearly to approximately 0.6° at 6° eccentricity (Smith, Singh, Williams, & Greenlee, 2001).

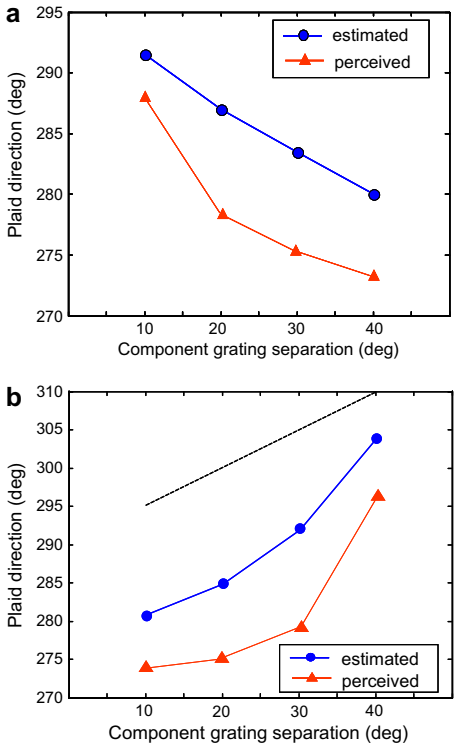

Fig. 3. Results from simulations of the computational model for the plaids used in the experiments of Burke and Wenderoth (1993), showing in a and b both the perceived plaid direction obtained in the experimental study (▲ symbols) and the plaid direction estimated by the model (● symbols). In Fig. 3a the mean component direction is 295°, and in Fig. 3b this direction varies and is shown by the dashed line. The graphs a and b show that the plaid direction estimated by the model varies with the difference in component grating direction and displays in both cases the same trend in the variation as observed in the Burke and Wenderoth (1993) study, although with a slightly greater bias towards the mean component direction of up to 9°. From the original diagram for the experimental results in this study, perceived errors were in the region of ±3°.

Since our results closely match the experimental results in each of these experiments, we can infer that our model results are robust if the 10 × 10 pixel window represents a receptive field diameter of between 0.15° and 0.6°, which is the approximate physiological range for V1 cells.

Our model breaks down when the simple algorithm we use to calculate the image intensity derivatives fails to produce acceptably accurate results. This happens when the spatial frequency of the stimulus is sufficiently high that the spatial period falls within a single window, i.e. is less than 10 pixels, corresponding to a frequency of 0.1 cycles/pixel, or between 6.7 cycles/° (corresponding to window size of 0.15° and a stimulus aperture diameter of 3°) and 1.6 cycles/° (corresponding to a window size of 0.6° and a stimulus aperture diameter of 12°). Thus, for the simulations of the Alais et al. (1997) experiments described in the Section 4, in which the aperture diameter is 3°, we did not simulate the result for a stimulus of 6 cycles/°.

It is important to note that the parameters of the model were held constant for all the simulation results described in this Section, i.e. for the Yo and Wilson (1992), the Bowns (1996), and the Burke and Wenderoth (1993) experiments.

4. Discussion

The original two-stage model (Adelson & Movshon, 1982; Movshon et al., 1985) has dominated research in plaid motion perception for almost 30 years, leading to an almost universal view that the first stage of plaid motion analysis involves the detection of the 1-D motion of the component gratings, carried out by component-direction selective neurons in V1 (see the review by Pack and Born (2008)). It is important to note however that the available evidence is almost entirely based on using symmetric Type I plaids, in which the component gratings move with equal speeds. For the psychophysical experiments of Movshon et al. (1985) the difference in directions of the component gratings was 120°, for their physiological experiments in cat and monkey V1 and in monkey MT (Movshon et al., 1985) the angular difference was 90°, and for Movshon and Newsome's (1996) physiological experiments in monkey V1 the difference was 90° or 45°. For such plaids, a neuron in primary visual cortex (V1) which responds optimally to the motion of a single grating, produces little response to a plaid moving in its optimal direction, as would be predicted from the orientations of the component gratings if the neurons were only responding to the 1-D motion of the gratings (Movshon et al., 1985). Our proposed model suggests that neurons in V1 respond both the 1-D and 2-D motion of the blob features of the plaid, and in the case of Type II plaids are driven by the 1-D edges and 2-D end-points of the elongated blobs. Moreover, we suggest that the 2-D motion is detected by end-stopped cells in V1, as observed by Pack et al. (2003). As we have discussed above, this model leads to theoretical and simulation results which closely mimic the physiological observations of perceived direction for such plaids. So how does the model explain the component-selective responses for V1 neurons in the case of Type I plaids, as observed by Movshon et al. (1985) and Movshon and Newsome (1996), in particular as the neurons observed by Movshon and Newsome (1996) were apparently mostly of the end-stopped variety ?

For Type I plaids in which the difference in the component grating directions is 90°, the blobs take the form of small square regions of high luminance which are aligned in the same orientations as the component gratings. Therefore, a neuron which is optimally responsive in the direction of the plaid motion, and with a long, narrow receptive field oriented orthogonally to the plaid direction, will respond sub-optimally to the two lines of blobs, each moving at 45° to the optimal direction for the neuron, in exactly the same way as if it were responding to the component gratings themselves, as shown by Tinsley et al. (2003). Little or no 2-D motion signal in the direction of the plaid would be detected due to the absence of well defined end-points in the stimulus, in contrast to the case of Type II plaids with elongated blobs. It is significant however that Movshon and Newsome (1996) observed a degree of pattern-selective response in two of the nine neurons they measured. Thus, we suggest, for such neurons and for symmetric Type I plaids, it is not possible to distinguish whether the neurons are responding to the component gratings or to the lines of small square blobs (which we will refer to as blob-lines) present in the plaid moving in the same directions as the component gratings. The lines formed by the blobs are certainly more perceptually salient to the human observer than the individual component gratings.

In our model, the outputs of the local motion detectors signalling the two orthogonal 1-D motions of the blob-lines described above will be combined in the second stage by the estimation algorithm to yield the vector sum of these two motions, the direction of which corresponds exactly to the IOC direction of motion in the case of a Type I plaid. Note that no initial or steady-state perceived direction bias was observed for Type I plaids by Ferrera and Wilson (1990) or Yo and Wilson (1992). It is also possible that the 2-D motion of the individual blobs may be signalled by V1 neurons with short, wide receptive fields, as observed by Tinsley et al. (2003). The combination of the outputs of the 2-D motion detectors and the 1-D motion detectors in the second stage of the model would reinforce the computation of the velocity estimate in the true plaid direction.

In summary, we argue that for symmetric Type I plaids, with a difference between the component grating directions of around 90°, the 1-D motion detectors in V1 will respond in exactly the same way to the blob-lines as to the component gratings. Since the blob-lines and the component gratings are indistinguishable, in terms of their orientation, direction, spatial frequency and speed, it is thus impossible for any experiment with such Type I plaids to distinguish between a model in which the first stage responds to the 1-D motion of the component gratings and one in which the first stage responds to the 1-D motion of the blob-lines. Since, in addition, the direction of a symmetric Type I plaid is given by the simple averaging (vector average) of the 1-D motion directions, it is impossible to distinguish between a model in which the second stage computes the IOC direction from one in which the second stage computes the vector average direction. We therefore conclude that the psychophysical experiments (Derrington & Badcock, 1992; Derrington & Suero, 1991; Welch, 1989) using symmetric Type 1 plaids, which have apparently confirmed the two-stage model of Adelson and Movshon (1982), are wholly inadequate in this respect. In contrast, the psychophysical experiments with Type II plaids (Yo & Wilson, 1992) strongly challenge the Adelson and Movshon model.

It is worth noting here that our theoretical analysis of the plaid blobs indicates, for asymmetric Type I plaids with an angular separation of component directions of >90° (e.g. the plaid in Fig. 1c), that a similar elongation of the blobs occurs, and that the longer edges increase in length as the angular separation increases. Also the orthogonal direction of the longer edges of the blobs approaches the vector sum direction of the component gratings. Hence our model predicts for such plaids a significant bias in the perceived direction of plaid motion towards the vector sum direction of the component gratings and away from the true IOC direction, of comparable magnitude to that observed for Type II plaids. As far as we are aware, no psychophysical or physiological experiments have been carried out for such Type I plaids.

A recent model of motion integration (Weiss & Adelson, 1998; Weiss et al., 2002) aimed at extending the Adelson and Movshon (1982) model to accommodate the Yo and Wilson (1992) results. According to Weiss and Adelson (1998) and Weiss et al. (2002), their model captures the uncertainty in the 1-D motion of the component gratings in the case of low contrast by using a Bayesian estimation process. The Bayesian formulation of the model results in the identification of a distribution of 1-D and 2-D velocity measurements which correspond to local likelihood functions. The model therefore represents the 1-D motion of each of the component gratings, corresponding to the first stage of the Adelson and Movshon model, as a pair of "fuzzy" (Weiss & Adelson, 1998) constraint lines in velocity space, the degree of fuzziness being dependent on contrast. The estimate of the plaid direction is then given by the mean/maximum of the posterior probability distribution, which is computed from the product of the local likelihoods and the prior distribution for the velocity estimate. The latter is assumed to be Gaussian with zero mean according to a "slow and smooth" (Weiss & Adelson, 1998; Weiss et al., 2002) hypothesis based on suggestions that human observers prefer the slowest motion consistent with the visual input (Ullman, 1979).

In fact, the model described by Weiss and Adelson (1998) and Weiss et al. (2002) is identical to the first step of the recursive Kalman filter estimation algorithm in our model, and therefore produces an identical, biased first step estimate of plaid direction. There appears therefore to be a contradiction between the explanation in Weiss and Adelson (1998) of the behaviour of the model in predicting plaid motion, which is solely in terms of the 1-D motion of the component gratings, and our explanation, which is in terms of the 1-D and 2-D motion of the edges and end-points blobs. The explanation in Weiss et al. (2002) is essentially the same as that in Weiss and Adelson (1998) but less detailed and with no supporting diagrams.

To resolve this contradiction, we first consider the plaid used to produce the simulation results shown in Fig. 2a, and previously discussed in Section 2.2. This plaid is also used in Weiss and Adelson (1998) and Weiss et al. (2002) as their main example for demonstrating the misperception of the direction of Type II plaids. The parameters of the component gratings of this plaid are, as given before: $\theta_1 = 70.5°$, $\theta_2 = 48.2°$, $r_1 = 1.33$, and $r_2 = 2.67$, yielding the following values: $\theta_1 - \theta_2 = 22.3°$, $\theta_{IOC} = 0.2°$, $r_{IOC} = 3.9$, $\theta_{VS} = 55.6°$, $r_{VS} = 4.0$, $\phi = 59.4°$, $r_\phi = 2.03$, $r_\varphi = 3.46$, $\phi - \theta_{VS} = 3.8°$ and $s_\phi / s_\varphi = 5.1$. For a contrast of 50%, our model calculates the initial estimate of the plaid velocity vector v_{e1} as: speed $r_{e1} = 1.84$ and direction $\theta_{e1} = 40°$.

Fig. 4a illustrates the plaid, clearly showing the elongated blobs. Fig. 4b is a velocity space diagram on which the velocity vectors of the component gratings, v_1 and v_2, together with their constraint lines, the initial velocity estimate, v_{e1}, and the IOC and vector sum velocity vectors, v_{IOC} and v_{VS} respectively, are shown (0° is vertically upward in this diagram). The velocity space diagram in Fig. 15d of Weiss and Adelson (1998) is redrawn as an inset in Fig. 4b.

In their Fig. 15d, the latter authors indicate the magnitude of the vector average (*VA*) velocity of the component gratings, rather than the vector sum velocity. Although the *direction* of these two velocity vectors are the same, the *magnitude (speed)* of the vector average velocity is half that of the vector sum velocity.

Weiss et al. (2002) explain the bias in the perceived direction towards the vector sum/average direction by the statement that "the vector average velocity [speed] is much slower than the IOC solution and hence it is favored [by the zero prior] at low contrasts". They assume that the Bayes estimate of plaid velocity is based on "local likelihoods [which] are 'fuzzy' constraint lines" (Weiss & Adelson, 1998) defined by the component grating velocities. Thus any bias in the estimate towards a speed slower than the IOC speed, as a consequence of the zero prior, will automatically result in a shift of the direction of the estimated velocity away from the IOC direction and towards the vector sum/average direction, i.e. the velocity estimate will be constrained to fall along, or close to, the dashed line depicted in Fig. 4b.

The explanation of the perceived direction bias in Weiss et al. (2002) and Weiss and Adelson (1998) is thus based on the Adelson and Movshon (1982) model of plaid perception, in which only the 1-D motion of the component gratings are detected in the first stage of analysis of the plaid motion, and their model is presented as a Bayesian extension of this model. This is clearly reflected in their explanation since they indicate that their model forms local likelihoods as "fuzzy" constraint lines defined by the 1-D motion of the component gratings. However their model, as ours, undoubtedly detects both the 1-D and 2-D motion that is present in the stimulus in the form of the motion of the edges and end-points of the blobs, as is clearly demonstrated by their depiction (in Fig. 3 of Weiss et al. (2002)) of the likelihood functions generated by their model for a moving diamond stimulus. It is surprising therefore that no reference is made to the likelihood functions formed from the 2-D motion in the plaid stimulus, and their role in forming the estimate.

We offer here an alternative explanation for the perceived plaid motion, which is based on the 1-D and 2-D motion of the edges and end-points of the blobs. This is illustrated in Fig. 4c. Here we show the velocity vectors corresponding to the orthogonal motion of the longer and shorter edges of the blobs in the plaid,

$$v_\phi \triangleq \begin{bmatrix} r_\phi \cos\phi \\ r_\phi \sin\phi \end{bmatrix}, \; v_\varphi \triangleq \begin{bmatrix} r_\varphi \cos\varphi \\ r_\varphi \sin\varphi \end{bmatrix}$$

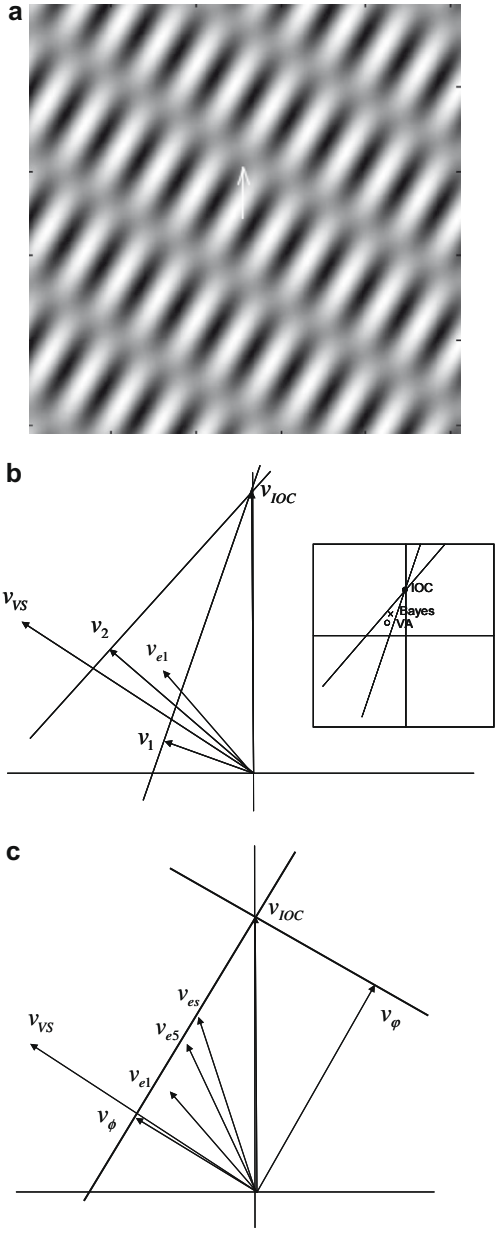

Fig. 4. Velocity space diagrams of the plaid used in the experiments of Yo and Wilson (1992) and for which the model simulation results are shown in Fig. 2a. (a) diagram illustrating the plaid, clearly showing the elongated blobs; (b) velocity space diagram on which the velocity vectors, v_1 and v_2, of the component gratings, together with their constraint lines, the IOC and vector sum velocity vectors v_{IOC} and v_{VS}, and the velocity estimate from our model for the first step, v_{e1}, are shown (0° is vertically upward in this diagram). The inset diagram is redrawn from Fig. 15d of Weiss and Adelson (1998); and (c) velocity space diagram showing the velocity vectors corresponding to the motion of the longer and shorter edges of the blobs in the plaid, v_ϕ and v_φ, together with their constraint lines, the IOC and vector sum velocity vectors, and the velocity estimates from our model for the first step, v_{e1}, the fifth step v_{e5}, and in the steady-state v_{es}. An explanation of the diagrams is given in the text.

respectively, and their constraint lines, together with the IOC and vector sum velocities, v_{IOC} and v_{VS} respectively, of the component gratings. Also shown are the velocity estimates from our model for the first step ($v_{e1} = 1.83$; $\theta_{e1} = 40°$), the fifth step ($v_{e5} = 2.38$; $\theta_{e1} = 25°$), and in the steady-state ($v_{es} = 2.62$; $\theta_{es} = 18°$).

It is clear that the initial estimate v_{e1} lies very close to the velocity vector v_ϕ, corresponding to the orthogonal motion of the long edge of the blob, and to the maximum of the likelihood function (the "fuzzy" constraint line) for v_ϕ. Subsequent velocity estimates in further iterations of the recursive algorithm get closer to this maximum, and also to the velocity vector v_{IOC}. Note that the effective prior for each step in the estimation algorithm is given by the velocity estimate in the previous step, which together with the influence of the likelihood function corresponding to the 2-D velocity of the end-points of the blobs, v_{IOC}, leads to the convergence of the estimate towards the IOC velocity.

To reinforce our account of the model behaviour, we provide a further piece of evidence that the first stage of plaid motion perception is based on the 1-D and 2-D motion of the blobs rather than the 1-D motion of the component gratings. Stone et al. (1990) investigated the effect on the perceived plaid direction of making the contrasts of the component gratings unequal. They based their investigation on the Adelson and Movshon (1982) model, assuming their first stage in which the 1-D velocities of the component gratings were detected to be correct. They hypothesised that the low contrast grating would be detected at a lower speed than the true value and that if this erroneous value were used in a second stage IOC calculation of plaid direction, a significant contrast-dependent error in the perceived plaid direction would result. They used a Type I plaid with angular separation of the component gratings of 120°, and changes in the ratio of the speeds of the component gratings to vary the true direction of the plaid whilst maintaining a constant plaid speed. In this way they found that the perceived plaid direction was biased towards the direction of the higher contrast grating and this bias increased for increasing contrast ratio, and also for decreasing total contrast (the sum of the grating contrasts). At 5% total contrast, the average observed bias varied between 0°, at a contrast ratio of 1, to ~16°, at a contrast ratio of 4:1. A maximum bias of 20° was observed for a total contrast of 10% and a contrast ratio of 8:1. The modified Adelson and Movshon (1982) model proposed by Stone et al. (1990) using perceived rather than actual component speeds appeared to give qualitatively similar results to those observed (see their Fig. 11). However, similar experiments by Champion et al. (2007) appeared to invalidate the modified IOC model of Stone et al. (1990), since it would also predict a bias towards the direction of the low contrast component at high component grating speeds due to an increase in the perceived speed of low contrast gratings for grating speeds above ~12 °/s (Champion et al., 2007). Champion et al. observed an increasing bias with component speed which was always towards the direction of the high contrast component except for the very lowest component grating speeds, but a *decrease* in the bias at the highest component speeds (above 12 °/s), consistent with their observed switch in the contrast-related misperception of grating speed for higher speed gratings. It should be noted however that Champion et al. used plaids of total contrast equal to 90%, compared to the total contrast values of between 5% and 40% used by Stone et al. They also used component gratings with angular separation of 90°, compared with the 120° angular separation used by Stone et al. Champion et al. also suggest that their results are inconsistent with the Bayesian IOC model of Weiss et al. (2002), since that model relies upon the perceived speed of the gratings being smaller for lower contrast, and hence higher uncertainty, owing to the greater influence of the "slow" prior. Champion et al. also claim that their results are inconsistent with several other models of plaid perception including the 1-D and 2-D parallel pathways model of Wilson et al. (1992), and the blob tracking model of Alais et al. (1994).

Applying our model to this data shows that it replicates the misperception of the direction of plaid motion towards the direction of the higher contrast grating, but the magnitude of the bias in the estimated direction is dependent on the spatial frequency of the component gratings. The case of a plaid with a separation of component gratings of 120°, 60° either side of the vertical (0°)

and a contrast ratio of 4:1 is shown in Fig. 5a. It is clear that the salient feature of this plaid is a set of blob-lines which are formed from a joining-up of the plaid blobs. The direction of motion of the blobs is the IOC direction of the component gratings, i.e. the plaid direction of 0°, but the orthogonal direction of motion of the blob-lines is 300°, the direction of the higher contrast component grating. The estimated plaid direction computed by our model is 308°, giving a bias of 52° away from the IOC direction of 0° towards the higher contrast grating direction, much greater than that measured by Stone et al. (1990), where the direction error was up to 20° for this contrast ratio (4:1). However, our result was obtained for a grating spatial frequency and a viewing aperture shown for the plaid illustrated in Fig. 5a, corresponding to ~14 cycles of the component gratings being present within the viewing aperture. If the gratings' spatial frequency and the viewing aperture are changed to approximate that used by Stone et al. (1990) and Champion et al. (2007), approximately six cycles of the component gratings are present in the viewing aperture, as illustrated by the plaid in Fig. 5b. The blob-lines are still clearly visible but the size of the blobs is greater by about a factor of two. In this case, the estimated plaid direction computed by our model is 342°, giving a bias towards the direction of the higher contrast grating of 18°, comparable to that measured by Stone et al. (1990) for this contrast ratio (4:1). The bias computed by our model for the contrast ratio of 2:1 was 7°, which is consistent with the Stone et al. result of approximately 7° for the 5% contrast case, and with the results of Champion et al. (2007) who used a contrast ratio of 2:1 and obtained a maximum bias of approximately 7°.

The above example illustrates the importance, both in psychophysical experiments and in modelling, of the choice of the spatial frequency of the component gratings in relation to the viewing angle/aperture of the stimulus. Our model results would suggest that if the psychophysical experiments of Stone et al. (1990) or Champion et al. (2007) had been carried out using a higher component grating spatial frequency, a far greater bias towards the higher contrast grating would have been obtained, owing to the greater salience of the 1-D motion of the blob-lines in the direction of the higher contrast grating, compared to that of the 2-D motion of the blobs themselves, when viewing the plaid.

Alais et al. (1997) investigated the effect of blob size and number on perceived plaid direction, in this case for Type II plaids. They showed, by varying both spatial frequency and viewing aperture size, that there is a large effect of blob size on the perceived direction bias, of up to 14.1°, due to changes in the component spatial frequency, but a small effect of blob number, of about 5°, obtained by changing aperture size whilst spatial frequency is held constant. We simulated their experiments with our model, keeping the viewing aperture constant and varying the spatial frequency of the component gratings. We used three values of spatial frequency: 0.6, 0.3 and 0.2 cycles/pixel. For the sake of comparing our simulation results with the experimental results, we assumed that these spatial frequencies corresponded to the experimental values of 3.0, 1.5, and 1.0 cycles/°.

We show in Fig. 6 the results from Alais et al. (1997) (their Fig. 5) giving the perceived direction as a function of spatial frequency for the 3° aperture case (● symbols), together with the steady-state direction estimates from the model (▲ symbols), for each of the component grating spatial frequencies. We do not simulate the 6.0 cycles/° owing to the limitations of our model in dealing with such high frequencies due to our choice of window size. As can be seen from Fig. 6, the estimates of the plaid direction are very similar to the perceived experimental values and, importantly, show the same trend, with a decrease in the misperceived direction bias as the spatial frequency of the component gratings increases.

It is not clear how a model of plaid perception based on the Adelson and Movshon (1982) model might account for the dependence of the misperception of plaid direction on component grating spatial frequency, as observed by Alias et al. (1997) and modelled by us. Varying the spatial frequency of the component

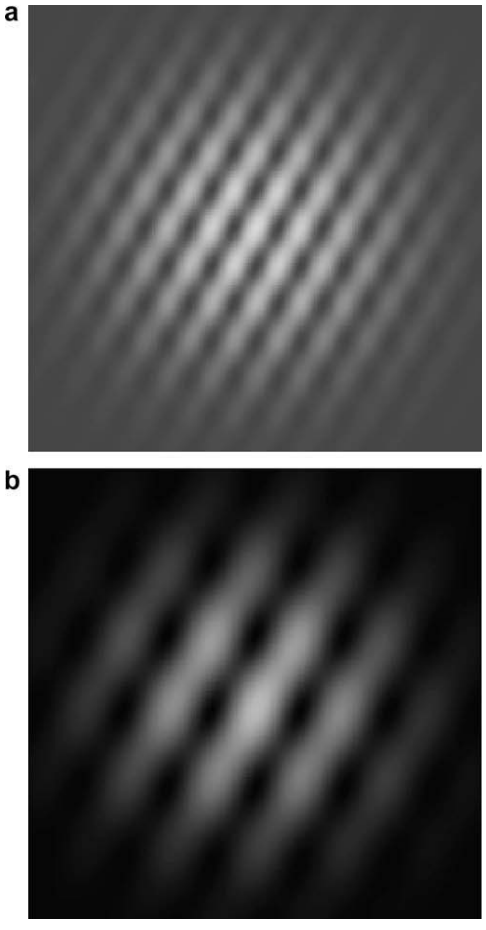

Fig. 5. The two plaids used the model simulations of the experiments of Stone et al. (1990), showing the effect of the spatial frequency of the component gratings on blob size and number. Both plaids correspond to an angular separation of component gratings of 120°, 60° either side of the vertical (0°) and for each the contrasts of the component gratings are in the ratio of 4:1. For the plaid in a. the spatial frequency of the component gratings is twice that for the plaid in b.

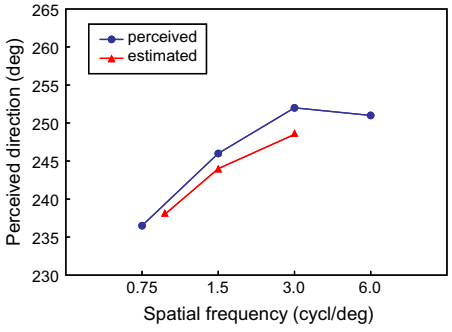

Fig. 6. Results from simulations of the computational model for the plaids used in the experiments of Alais et al. (1997) showing the perceived plaid direction as a function of spatial frequency obtained in the experimental study, for the 3° aperture case (▲ symbols) and the plaid direction estimated by the model (● symbols). The estimates of the plaid direction are very similar to the perceived values (within 4°) and show the same trend, with a decrease in the misperceived direction bias as the spatial frequency of the component gratings increases. From the original diagram for the experimental results in this study, perceived errors were in the region of ±2°.

gratings should have no effect on the computation of the 1-D velocity of the gratings, or on the IOC calculation, even in the case of where uncertainty in the component directions is taken into account as in the Bayesian IOC model of Weiss et al. (2002) and Weiss and Adelson (1998). On the other hand, our model, which depends on both the 1-D and 2-D motion of the blobs, is entirely consistent with the Alais et al. (1997) results. As noted by them: "These results provide further support for the existence of a feature-sensitive mechanism which responds to the motion of plaid features and which is tuned to their various qualities". Our model provides just such a mechanism.

Other approaches based on a feature tracking mechanism have been proposed which are related to the mechanisms that we have described here. In particular, Bowns (1996) proposed a feature tracking explanation for the misperception of Type II plaids as observed by Yo and Wilson (1992) which is based on specific plaid features, "avgL", "minL" and "maxL" which she introduces, and which clearly relate to the blob features that we have defined in Section 2.

In Fig. 6 of Bowns (1996), these features and their motion are illustrated for a plaid in which the directions of motion of the two component gratings differ by 10° (directions of 90° and 100°). According to our analysis, the blobs in this plaid, which appear to correspond approximately in shape to the maxL feature, have an edge ratio of 1:0.09, i.e. the blobs are highly elongated, and the longer edges move in an orthogonal direction of 95°, almost exactly equal to the vector sum direction of 93°. For a component grating speed ratio of 1:0.5, our model gives for this plaid an initial direction estimate of 90° and a final direction estimate of 65°, i.e. 25° to the right hand (IOC = 19°) side of the vertical, implying that in a forced choice decision of left or right of the vertical, as in the Bowns (1996) experiments, a consistent IOC choice would be likely. At this point we refer the reader back to our description and simulations of Bowns' 1996 experiments in Section 3.1. A different explanation is however given in Bowns (1996) for consistent IOC result; namely that, as stated in the legend to Fig. 6 "there are no edges that move in the vector sum direction for this plaid". Hence it is concluded that the choice will always be in the IOC direction.

In Fig. 7 of Bowns (1996), avgL, maxL and minL are again illustrated for a plaid in which the directions of motion of the two component gratings differ by 80° (directions of motion of 90° and 170°). In the legend to the figure it is stated again that "there are no edges that move in the vector sum direction for this plaid". However, for this plaid our analysis shows that the blobs are not elongated, having an edge ratio of 1:0.84, which would predict a velocity estimate close to the IOC direction. Also for this a plaid, the IOC direction (108°) is close to the vector sum direction (114°), and both are thus to the left of the vertical. Our model gives initial and final velocity estimates for this plaid which are both approximately equal to the IOC direction, thus predicting, in a forced choice of left or right of the vertical, a decision of left (vector sum), corresponding to the outcome in the actual experiment, as indicated in the legend to Fig. 7 of Bowns (1996).

Finally, in Fig. 8 of Bowns (1996), avgL, maxL and minL are illustrated for a plaid in which the directions of motion of the two component gratings differ by 40° (directions of motion of 90° and 130°). In this case, the legend to Fig. 8 indicates that whilst neither of the features maxL or minL have edges moving in the vector sum direction, avgL has an edge which moves in this direction. The inference is made that the presence of this motion resulted in subjects performing variably with this plaid, one perceiving it in the IOC direction (right of the vertical) and one in the vector sum direction (left of the vertical). From our analysis, for this plaid, and a speed ratio of 1:0.5, the blob edge ratio is 1:0.36, i.e. the blobs are somewhat elongated, and their long edges move in an orthogonal direction of 110°, close to the vector sum direction of 103°.

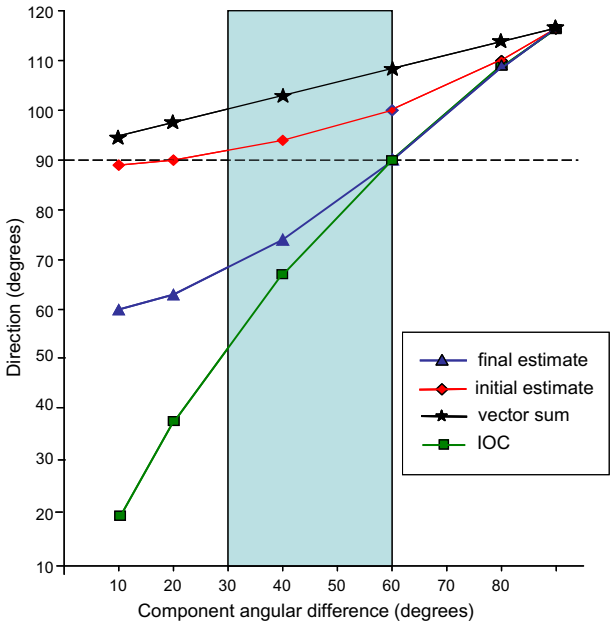

Fig. 7. Results from simulations of the computational model for the plaids used in Experiment 2 of Bowns (1996), showing the initial and final estimated plaid directions as a function of the angular difference between the component grating directions for these plaids. The shaded area in the centre of the graph indicates those component grating angular differences which resulted in an inconsistent choice by subjects between "vector sum direction" and "IOC direction" for the corresponding plaids (see the text in the Section 4 for a further discussion of these results).

Our model estimates a plaid velocity direction in the first step of the estimation algorithm of 95° (5° to the left of the vertical) and a final estimate of 73° (17° to the right of the vertical). The IOC direction is 67°.

The results from our simulations of the full range of plaids used in Experiment 2 of Bowns (1996), of which those discussed above are a subset, are shown in Fig. 7. The plots in Fig. 7 show the initial and final estimated plaid directions as a function of the angular difference between the component grating directions for these plaids. The shaded area in the centre of the graph indicates the range of component grating angular differences which resulted in an inconsistent choice by subjects between "vector sum direction" and "IOC direction" for the corresponding plaids. From these results, and our discussion above, we suggest that the reason for the observed variability between subjects in their choice of IOC or vector sum direction (Bowns, 1996) lies in the variability of subjects in terms of the dependence of their direction perception on the duration of the stimulus. As Yo and Wilson (1992) showed, subjects can display considerable differences in this dependence. In Fig. 6 of Yo and Wilson, one subject (HRW) reported a direction bias of 30° after ~90 ms stimulus duration, from an initial bias of ~60° at 60 ms. Another subject (HJ) reported a direction bias of 15° after ~90 ms, from approximately the same initial bias at 60 ms. Significantly, the stimulus duration used in the Bowns (1996) experiments was 80 ms, which would imply that a significant variation in perceived bias between subjects at this duration was possible. A similar variability to that reported by Yo and Wilson (1992) would therefore probably be sufficient to cause the difference in direction choice between the two subjects in the Bowns (1996) experiments.

Whilst our explanation contrasts with that of Bowns (1996), her explanation does clearly indicate that there is present in the plaid pattern both motion in the vector sum direction (in our analysis the orthogonal 1-D motion of the longer edges of the blobs) and

in the IOC direction (in our analysis the 2-D motion of the blob end-points). She uses this fact to propose that the variation between subjects may result from a competition between these two sets of motion information. Our analysis suggests that a recursive Bayesian process which uses both information sets can also predict this result.

Another analysis of Type II plaid misperception based of the motion of features in the plaid was presented in Bowns (2006). Here a squaring operation is performed on the plaid and two "components" are identified: "sqHF" and "sqLF" which are derived from the squared plaid. The description in Bowns (2006) shows that the "components" are in fact two gratings formed from the squared plaid pattern, a high spatial frequency grating and a low spatial frequency grating, with spatial frequencies and orientations defined in the Appendix. They clearly relate to the product gratings, and have the same orientations and direction of motion as these, as illustrated in Fig. 1d of Bowns (2006). Examples of the values for the direction of motion of the sqHF and sqLF are also given for three Type II plaids, which were also used in Bowns (1996), showing that the direction of motion of the sqHF "component" is close to the vector sum direction. This led to the proposal that the direction of motion of the "components" provided a better overall predictor of the misperceived direction of these plaids than either the vector sum, as suggested by Yo and Wilson (1992), or the IOC direction, as suggested by Adelson and Movshon (1982). We clearly concur with this conclusion, as our predictions based on the motion of the blob edges show. However, Bowns also suggests that there is no motion energy in the plaids in the IOC direction, so that a full explanation of the misperception would "a model that incorporates both squaring and the IOC". Our model however incorporates both the 1-D motion of the blob edges, which contain motion energy close to the vector sum direction, and the 2-D motion of the blob end-points, which contain motion energy in the IOC direction. Used together in a recursive Bayes estimation framework, we have shown that this model closely predicts a wide range of results on perceived direction of plaid motion.

In addition to providing plausible explanations for a wide range of existing psychophysical and physiological results, new directions for experimental investigation are suggested by our model, including monitoring the response to Type II plaid motion of end-stopped cells (Hubel & Weisel, 1965; Pack et al., 2003) in layer 4b of area V1, the layer which contains the majority of V1 neurons projecting to MT. We predict that such experiments will indicate that these neurons signal the 2-D motion of the high luminance regions in the plaid, for Type II plaids. Additionally, studies of the dynamic response of MT neurons to Type II plaids have, as far as we are aware, not been done, although a stimulus consisting of a field of short bright bars (Lorenceau, Shiffrar, Wells, & Castet, 1993) mimics the high luminance regions in Type II plaids. For this barfield stimulus, Pack and Born (2001) showed that MT neurons initially respond primarily to the component of motion perpendicular to a contour's orientation, but over a period of approximately 60 ms the responses gradually shift to encode the true stimulus direction, regardless of orientation. Thus the responses of the MT cells closely parallel the psychophysical responses of human observers to the motion of Type II plaids (Yo & Wilson, 1992). Similar studies in which the responses of MT neurons are selectively inhibited, by lesioning or reversibly cooling (Hupé et al., 1998; Supèr & Lamme, 2007) might also be able to test our hypothesis that the local 1-D and 2-D local motion signals are combined to provide the perception of plaid motion via a recursive estimation process, which we hypothesise is implemented in the recurrent interaction between V1 and MT, an interaction which has been strongly implicated in the perceptual awareness of visual motion (Lamme & Roelfsema, 2000; Sterzer, Haynes, & Rees, 2006)

Acknowledgement

The research reported here was partially supported by funding under the Sixth Research Framework Programme of the European Union under the Grant No. 15879 (FACETS).

References

Adelson, E. H., & Movshon, J. A. (1982). Phenomenal coherence of moving visual patterns. *Nature, 300*, 523–525.
Alais, D. M., Wenderoth, P. M., & Burke, D. C. (1994). The contribution of 1-D motion mechanisms to the perceived direction of drifting plaids and their aftereffects. *Vision Research, 34*, 1823–1834.
Alais, D. M., Wenderoth, P. M., & Burke, D. C. (1997). The size and number of plaid blobs mediate the misperception of Type-II plaid direction. *Vision Research, 37*, 143–150.
Bowns, L. (1996). Evidence for a feature tracking explanation of why Type II plaids move in the vector sum direction at short durations. *Vision Research, 36*, 3685–3694.
Bowns, L. (2006). Squaring is better at predicting plaid motion than the vector average or intersection of constraints. *Perception, 35*, 469–481.
Burke, D., & Wenderoth, P. (1993). The effect of interactions between one dimensional component gratings on two dimensional motion perception. *Vision Research, 33*, 343–350.
Champion, R. A., Hammett, S. T., & Thompson, P. G. (2007). Perceived direction of plaid motion is not predicted by component speeds. *Vision Research, 47*, 375–383.
Derrington, A. M., & Badcock, D. R. (1992). Two-stage analysis of the motion of 2-dimensional patterns: What is the first stage? *Vision Research, 32*, 691–698.
Derrington, A. M., & Suero, M. (1991). Motion of complex patterns is computed from the perceived motions of their components. *Vision Research, 31*, 139–149.
Derrington, A. M., & Ukkonen, O. I. (1999). Second-order motion discrimination by feature-tracking. *Vision Research, 39*, 1465–1475.
Dimova, K., & Denham, M. (2009). A neurally plausible model of motion integration in smooth eye pursuit based on recursive Bayesian estimation. *Biological Cybernetics, 100*, 185–201.
Fennema, C. L., & Thompson, W. B. (1979). Velocity determination in scenes containing several moving objects. *Computer Graphics and Image Processing, 9*, 301–315.
Ferrera, V., & Wilson, H. (1990). Perceived direction of moving two-dimensional patterns. *Vision Research, 30*, 273–287.
Ferrera, V., & Wilson, H. (1991). Perceived speed of moving two-dimensional patterns. *Vision Research, 31*, 877–893.
Hubel, D. H., & Weisel, T. N. (1965). Receptive fields and functional architecture in two nonstriate visual areas (18 and 19) of the cat. *Journal of Neurophysiology, 28*, 229–289.
Hupé, J. M., James, A. C., Payne, B. R., Lomber, S. G., Girard, P., & Bullier, J. (1998). Cortical feedback improves discrimination between figure and background by V1, V2 and V3 neurons. *Nature, 394*, 784–787.
Kalman, R. E. (1960). A new approach to linear filtering and prediction problems. *Transactions of the ASME Journal Basic Engineering, 82*, 35–45.
Lamme, V. A., & Roelfsema, P. R. (2000). The distinct modes of vision offered by feedforward and recurrent processing. *Trends in Neurosciences, 23*, 571–579.
Lorenceau, J., Shiffrar, M., Wells, N., & Castet, E. (1993). Different motion sensitive units are involved in recovering the direction of moving lines. *Vision Research, 33*, 1207–1217.
Marr, D., & Ullman, S. (1981). Directional selectivity and its use in early visual processing. *Proceedings of the Royal Society Series B-Biological Sciences, 211*, 151–180.
Masson, G. S., & Stone, L. S. (2002). From following edges to pursuing objects. *Journal of Neurophysiology, 88*, 2869–2873.
Movshon, J. A., Adelson, E. H., Gizzi, M. S., & Newsome, W. T. (1985). The analysis of moving visual patterns. In C. Chagas, R. Gattass, & C. Gross (Eds.), *Pattern recognition mechanisms* (pp. 117–151). New York: Springer.
Movshon, J. A., & Newsome, W. T. (1996). Visual response properties of striate cortical neurons projecting to area MT in macaque monkeys. *Visual Neuroscience, 16*, 7733–7741.
Pack, C. C., & Born, R. T. (2001). Temporal dynamics of a neural solution to the aperture problem in visual area MT of macaque brain. *Nature, 409*, 1040–1042.
Pack, C. C., & Born, R. T. (2008). Cortical mechanisms for the integration of visual motion. In A. I. Basbaum, Akimichi Kaneko, G. M. Shepherd, & G. Westheimer (Eds.). *The senses: A comprehensive reference, vision II* (Vol. 2, pp. 189–218). Thomas D. Albright and Richard Masland, Academic Press.
Pack, C. C., Livingstone, M. S., Duffy, K. R., & Born, R. T. (2003). End-stopping and the aperture problem: Two-dimensional motion signals in macaque V1. *Neuron, 39*, 671–680.
Smith, A. T., Singh, K. D., Williams, A. L., & Greenlee, M. W. (2001). Estimating receptive field size from fMRI data in human striate and extra-striate visual cortex. *Cerebral Cortex, 11*, 1182–1190.
Sterzer, P., Haynes, J. D., & Rees, G. (2006). Primary visual cortex activation on the path of apparent motion is mediated by feedback from hMT+/V5. *Neuroimage, 32*, 1308–1316.
Stone, L., Watson, A., & Mulligan, J. (1990). Effect of contrast on the perceived direction of a moving plaid. *Vision Research, 30*, 1049–1067.

Supèr, H., & Lamme, V. A. (2007). Altered figure-ground perception in monkeys with an extra-striate lesion. *Neuropsychologia, 45*, 3329–3334.
Tinsley, C. J., Webb, B. S., Barraclough, N. E., Vincent, C. J., Parker, A., & Derrington, A. M. (2003). The nature of V1 neural responses to 2D moving patterns depends on receptive field structure in the marmoset monkey. *Journal of Neurophysiology, 90*, 930–937.
Ullman, S. (1979). *The interpretation of visual motion*. Cambridge: MIT Press.
Wallace, J. M., Stone, L. S., & Masson, G. S. (2005). Object motion computation for the initiation of smooth pursuit eye movements in humans. *Journal of Neurophysiology, 93*, 2279–2293.
Wallach, H. (1935). Ueber visuell whargenommene bewegungrichtung. *Psychologische Forschung, 20*, 325–380.
Weiss, Y., & Adelson, E. H. (1998). *Slow and Smooth: a Bayesian theory for the combination of local motion signals in human vision*. Massachusetts Institute of Technology, Dept. of Brain and Cognitive Sciences, A.I. Memo. No. 1624.
Weiss, Y., Simoncelli, E. P., & Adelson, E. H. (2002). Motion illusions as optimal percepts. *Nature Neuroscience, 5*, 598–604.
Welch, L. (1989). The perception of moving plaids reveals two processing stages. *Nature, 337*, 734–736.
Wenderoth, P. M., Alais, D. M., Burke, D. C., & van der Zwan, R. (1994). The role of "blobs" in determining the perception of drifting plaids and motion aftereffects. *Perception, 23*, 1163–1169.
Wilson, H. R., Ferrera, V. P., & Yo, C. (1992). A psychophysically motivated model for two-dimensional motion perception. *Visual Neuroscience, 9*, 79–97.
Wilson, H. R., & Kim, J. (1994). A model for motion coherence and transparency. *Visual Neuroscience, 11*, 1205–1220.
Wuerger, S., Shapley, R., & Rubin, N. (1996). "On the visually perceived direction of motion" by Hans Wallach: 60 years later. *Perception, 25*, 1317–1367.
Yo, C., & Wilson, H. (1992). Perceived direction of moving two-dimensional patterns depends on duration, contrast, and eccentricity. *Vision Research, 32*, 135–147.